ANL-LTR-NEAMS-10-001

FY10 Report on Multi-scale Simulation of Solvent Extraction Processes: Molecular-scale and Continuum-scale Studies

Chemical Sciences and Engineering Division

About Argonne National Laboratory

Argonne is a U.S. Department of Energy laboratory managed by UChicago Argonne, LLC under contract DE-AC02-06CH11357. The Laboratory's main facility is outside Chicago, at 9700 South Cass Avenue, Argonne, Illinois 60439. For information about Argonne and its pioneering science and technology programs, see www.anl.gov.

Availability of This Report

This report is available, at no cost, at http://www.osti.gov/bridge. It is also available on paper to the U.S. Department of Energy and its contractors, for a processing fee, from:

U.S. Department of Energy
Office of Scientific and Technical Information
P.O. Box 62
Oak Ridge, TN 37831-0062
phone (865) 576-8401
fax (865) 576-5728
reports@adonis.osti.gov

Disclaimer

This report was prepared as an account of work sponsored by an agency of the United States Government. Neither the United States Government nor any agency thereof, nor UChicago Argonne, LLC, nor any of their employees or officers, makes any warranty, express or implied, or assumes any legal liability or responsibility for the accuracy, completeness, or usefulness of any information, apparatus, product, or process disclosed, or represents that its use would not infringe privately owned rights. Reference herein to any specific commercial product, process, or service by trade name, trademark, manufacturer, or otherwise, does not necessarily constitute or imply its endorsement, recommendation, or favoring by the United States Government or any agency thereof. The views and opinions of document authors expressed herein do not necessarily state or reflect those of the United States Government or any agency thereof, Argonne National Laboratory, or UChicago Argonne, LLC.

ANL-LTR-NEAMS-10-001

FY10 Report on Multi-scale Simulation of Solvent Extraction Processes: Molecular-scale and Continuum-scale Studies

prepared by
Kent E. Wardle, Kurt Frey, and Candido Pereira
Chemical Sciences and Engineering Division, Argonne National Laboratory

September 30, 2010

work sponsored by
U.S. Department of Energy,
Office of Nuclear Energy, Science and Technology

FY10 Report on Multi-scale Simulation of Solvent Extraction Processes: Molecular-scale and Continuum-scale Studies

Kent E. Wardle, Kurt Frey, and Candido Pereira
Argonne National Laboratory

This task is aimed at predictive modeling of solvent extraction processes in typical extraction equipment through multiple simulation methods at various scales of resolution. We have conducted detailed continuum fluid dynamics simulation on the process unit level as well as simulations of the molecular-level physical interactions which govern extraction chemistry. Through combination of information gained through simulations at each of these two tiers along with advanced techniques such as the Lattice Boltzmann Method (LBM) which can bridge these two scales, we can develop the tools to work towards predictive simulation for solvent extraction on the equipment scale (Figure 1). The goal of such a tool—along with enabling optimized design and operation of extraction units—would be to allow prediction of stage extraction efficiency under specified conditions. Simulation efforts on each of the two scales will be described below. As the initial application of FELBM in the work performed during FY10 has been on annular mixing it will be discussed in context of the continuum-scale. In the future, however, it is anticipated that the real value of FELBM will be in its use as a tool for sub-grid model development through highly refined DNS-like multiphase simulations facilitating exploration and development of droplet models including breakup and coalescence which will be needed for the large-scale simulations where droplet level physics cannot be resolved. In this area, it can have a significant advantage over traditional CFD methods as its high computational efficiency allows exploration of significantly greater physical detail especially as computational resources increase in the future.

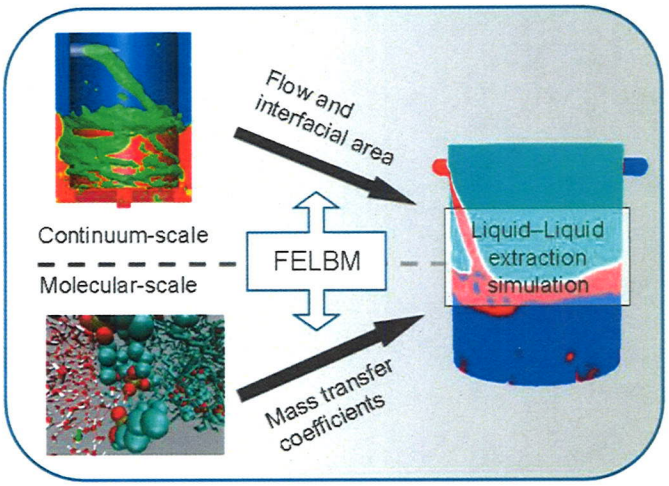

Figure 1. Depiction of multi-scale simulation effort.

Molecular-scale Simulations: Development of Polarizable TBP Model

The goal of the molecular modeling efforts was to begin exploration of the application of advanced inter-molecular potentials incorporating polarizability for solvent extraction relevant systems. As a baseline for future polarizable simulations and to provide an equilibrated system configuration from which to begin those polarizable simulations, a number of simulations for the water/TBP/dodecane system were conducted using the standard, fixed partial charge model for tributyl phosphate (TBP) that was developed during FY09. From this work we determined an adequate initialization procedure to obtain sufficiently fast system equilibration and were able to observe extraction and subsequent clustering of water in the organic phase through interfacial interactions with TBP molecules. A preliminary polarizable model for TBP was also constructed

using *ab initio* calculations done with Gaussian along with a charge fitting routine in the CHarMM molecular dynamics code. A description of both the non-polarizable and polarizable developments follows.

Fixed Partial Charge MD Simulations of water/TBP/dodecane[1]

Simulations using all non-polarizable models were conducted using three different system initial configurations to determine the effect of the initial state on the speed of system equilibration and the equilibrated system state. It is desirable to provide an initial configuration that offers a fast pathway towards the equilibrated state—which in the case of the system under consideration means that TBP molecules, which will assist in water migration into the organic phase, should be near the liquid-liquid interface. Initial configurations and system setup was done using CHarMM version 36a2 and molecular dynamics simulations were done using NAMD 2.7.

In order to provide a comparison versus other initial configurations, a simulation was done using an organic phase in which the TBP was uniformly dispersed throughout. At time zero, the organic box and water box were placed side by side and a liquid-liquid interface forms. It was found that this case required a simulation time in excess of 50ns for TBP to migrate towards the interface and water to begin migration into the organic phase. Even at 50ns very little water migration was found to have occurred (Figure 2).

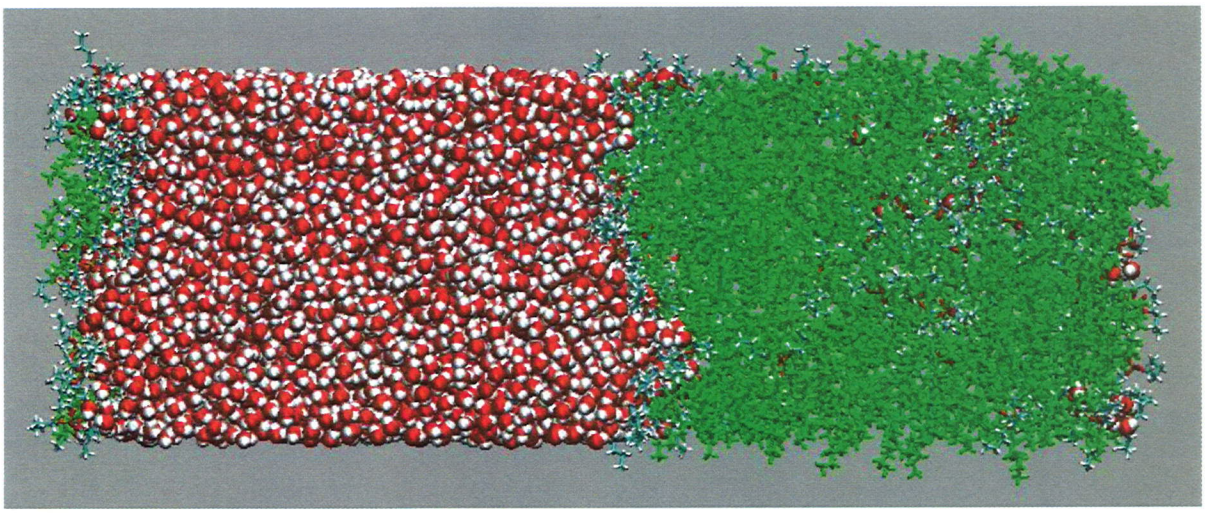

Figure 2. Snapshot of system state after 50ns of dynamics for simulation initialized from randomly mixed organic box. Water is shown as red and white spheres, dodecane as bright green tubes and TBP as multicolored tubes.

The other extreme in initialization would be to have all of the TBP in a layer at the interface. This too was tried and the model was extensively equilibrated though the results were somewhat unexpected. Instead of some TBP staying at the interface and some migrating out into the bulk, the TBP layer remained as a 'stable' phase of its own. Figure 3 shows a snapshot after 100ns of dynamics. Even after this relatively long simulation time, no TBP had migrated into the bulk dodecane. Apparently, a relatively stable 'third-phase' was formed due to the artificial interface

[1] Thanks to Brian Gullekson (Oregon State University) for his work as a summer intern on this portion of the project.

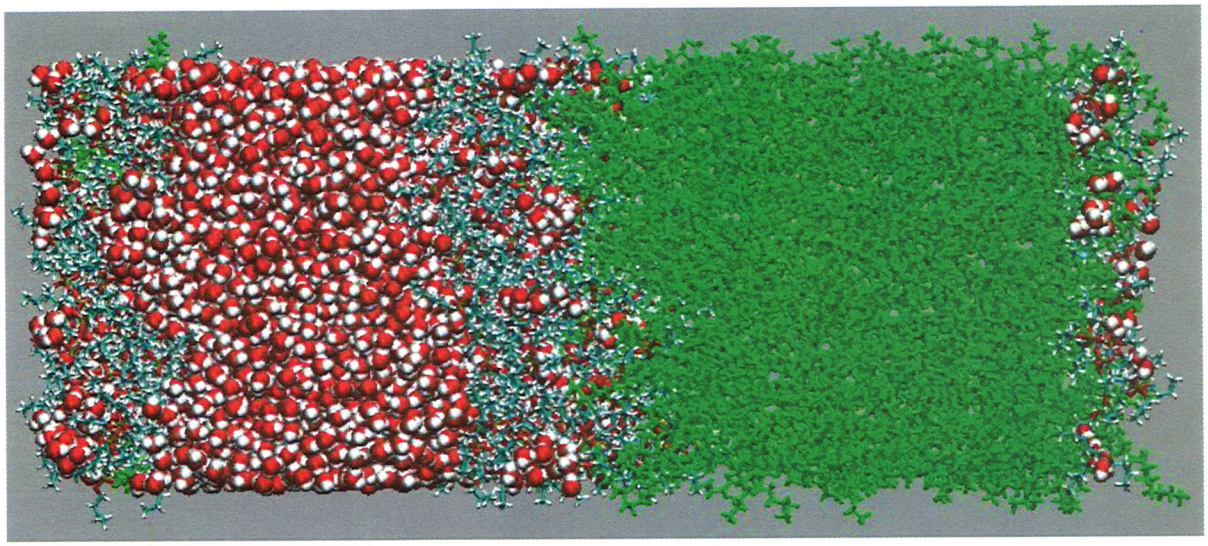

Figure 3. Snapshot of TBP layer initialized system after 100ns of dynamics showing a stable third-phase and no TBP migration into the bulk dodecane (green).

construction procedure. While third phase formation does occur experimentally in dodecane/TBP systems, it has only been observed for heavy solute loading of the organic phase and should not occur naturally for a 'clean' water system. Presumably this is a metastable state that will break down at later times.

A third system initialization procedure was found to give adequate results. This system was constructed with the TBP near the interface to eliminate the extra time required for its diffusion, but also with a small layer of dodecane in between the water box and TBP layer. The model had 6000 water, 704 dodecane, and 240 TBP molecules. This construction was proposed to allow TBP to diffuse into dodecane before interacting with water and eliminating the problem of a stable third-phase due to some moderate dodecane disruption of the interface layer. Even so, quick TBP saturation of the interface is likely to occur since the TBP molecules are placed near the interface. Indeed this was found to be the case as can be seen in the successive snapshots shown in Figure 4 at 10ns, 25ns, and 50ns after startup. In these snapshots it can be seen that the dodecane layer successfully disrupted the interface and allow TBP to begin dispersing and mixing with the bulk dodecane during the first stage of the simulations. Comparison of the 50ns snapshot for this system with Figure 2 shows the advantage of initialization of the TBP near the interface.

The stagewise progression of the simulation is, first, migration of TBP towards the interface takes place (10ns) followed by migration of water molecules (25ns), and finally clustering of water molecules (50ns). Without continuation of the simulation to longer times, it is unclear if subsequent migration of the water clusters and their accompanying TBP molecules into the bulk organic phase will occur. The water clusters and state of water migration into the organic phase is seen in the density profiles time-averaged over the last 10ns of the simulation as shown in Figure 5. The molecular density of water (red line) drops off from a level maximum in the bulk phase to zero in the middle of the organic phase (green line). The TBP surrounded clusters of water (micelles) are evident by the water plateaus seen at $z = -15$ and $z = -75$.

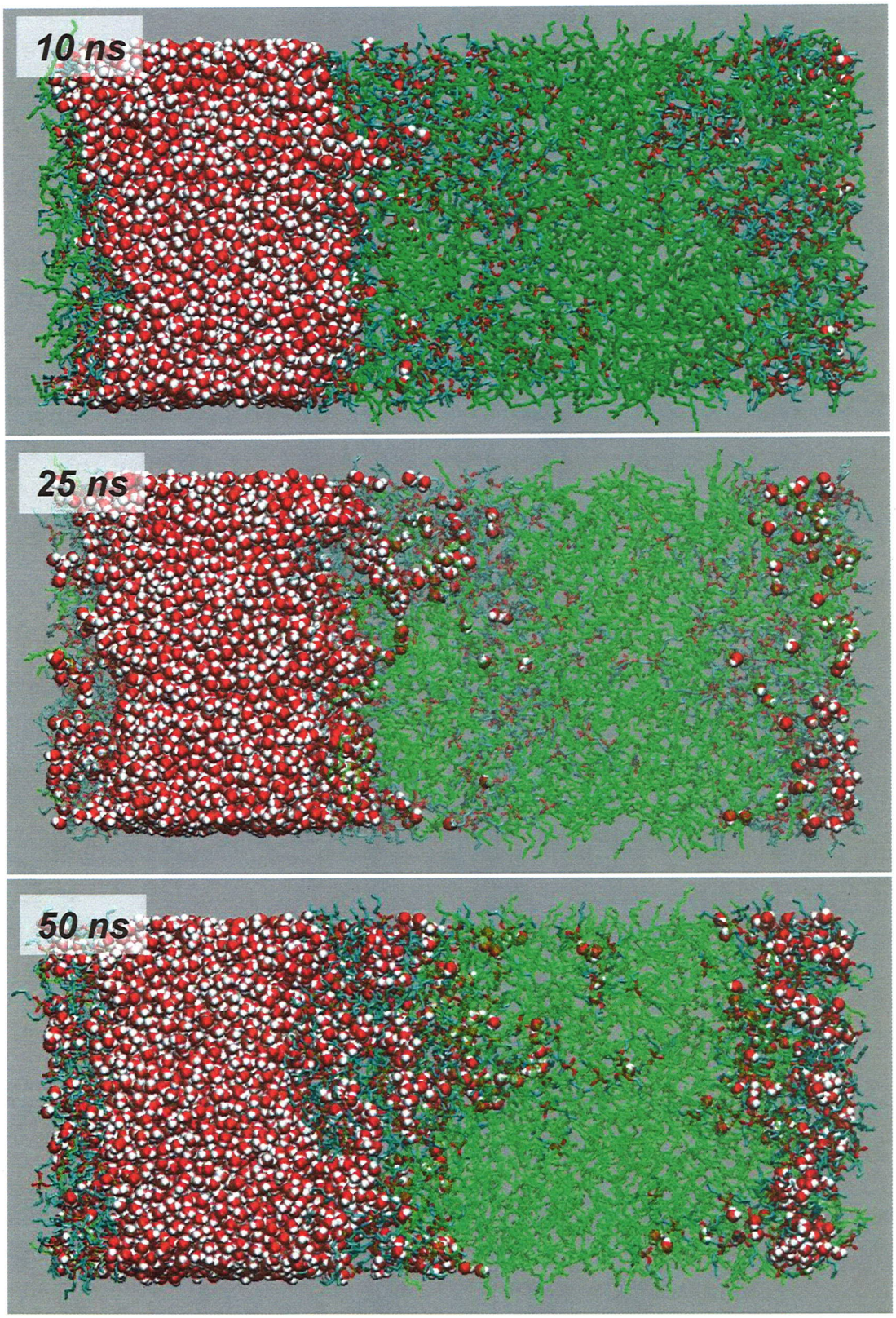

Figure 4. Snapshots at three different times after startup for the system initialized with a small layer of dodecane between the water and TBP layers. A progression from TBP migration, to water migration, and finally water clustering is evident.

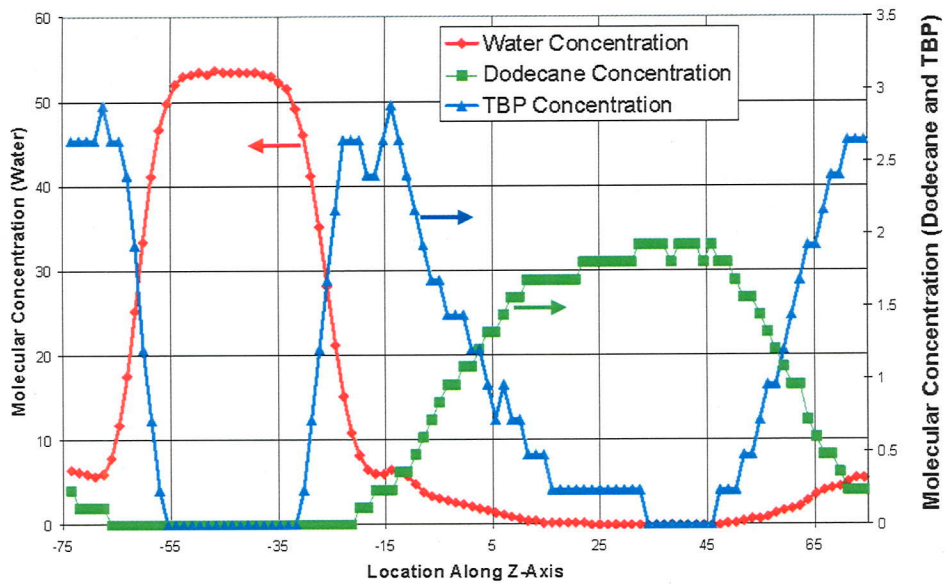

Figure 5. Density profile along the z-direction (normal to the interface) time-averaged over the last 10ns of the simulation.

It was concluded that this model and initialization procedure gave an adequate balance of ease of initialization and minimization of computational expense to achieve a physically realistic system. The final configuration from this simulation can be used in the future as the starting point for a simulation based on all polarizable models.

Polarizable TBP Model Development and Testing

Molecular models used in simulations such as those above typically involve fixed point charges located at atomic centers. These point charges help to account for the long-range Coulombic forces present within the system. However, by assigning these point charges to fixed locations at atomic centers, all rigid molecules are given a static electric dipole independent of the molecular environment. The electric charge in real systems is distributed continuously in three dimensions about atomic centers and not confined to discrete points. This continuous distribution responds dynamically to external electric fields, giving rise to an induced dipole (i.e., polarizability). For liquid systems, the magnitude of the induced dipole is of the same order as the static dipole, and should be incorporated into the molecular model to achieve greater predictive accuracy.

The Drude oscillator model is a method of accounting for polarizability aspects in a molecular representation of a system. Each of the atomic centers with a point charge in the original model (excluding hydrogen) is assigned an additional 'Drude particle'. These particles are tethered to their corresponding atomic centers using a harmonic oscillator with an equilibrium displacement of zero; in the absence of external forces, the Drude particles are coincident with their respective atomic centers. Each point charge is distributed between the atomic center and Drude center, so that in the presence of an external electrical field, a portion of the electrical charge will change position and give rise to an induced dipole. By convention, a uniform spring constant is used for all Drude particles (1000 kcal/mol/$Å^2$). Incorporating a Drude oscillator description into a molecular model requires determining the appropriate distribution of charges between the atomic centers and Drude particles.

Table 1. Polarizable model parameters for model developed with partial symmetry (V1.1) and full rotational symmetry (V1.2).

Model →	Version 1.1		Version 1.2	
Atomic Center	**Point Charge**	**Polarizability (-)**	**Point Charge**	**Polarizability (-)**
P	0.255 e	1.780 $Å^3$	0.297 e	1.980 $Å^3$
O=	-0.336 e	0.507 $Å^3$	-0.405 e	0.564 $Å^3$
-O-	0.020 e	0.570 $Å^3$	0.043 e	0.634 $Å^3$
-CH2-	0.105 e	1.638 $Å^3$	0.089 e	1.823 $Å^3$
-CH3	0.133 e	1.976 $Å^3$	0.113 e	2.199 $Å^3$
-H	-0.049 e	--	-0.043 e	--

Electronic structure calculations were performed on tributyl phosphate (TBP) using Gaussian, a computational chemistry software program. The response of the TBP molecule's electrostatic potential to thirty point charges was calculated. These response surfaces were used in a minimization routine incorporated in CHarMM, a molecular dynamics program, to optimize the charge distributions between the atomic centers and Drude particles. Although the TBP molecule involves 44 atomic centers, only six of these centers have unique values. Table 1 gives the values for two polarizable models the first calculated with partial symmetry (referred to as version 1.1) and the second with full rotational symmetry (version 1.2). The bond, angle, dihedral, and non-bonded model parameters were the same as used for the non-polarizable model and were taken from the Charmm27 forcefield.

Molecular dynamics simulations using the two models in Table 1 were conducted using NAMD 2.7. Simulation for a box of 144 TBP molecules (roughly ~45^3 $Å^3$) was done for the two models. Both simulations were run 1 ns for equilibration and 1 ns for averaging of data. The predicted density, self diffusion constant, molecular dipole, and dielectric constant were calculated and compared with the experimental values. All experimental values were taken from L.L. Burgess, "Chapter 3: Physical Properties" in *The Science and Technology of Tributyl Phosphate, Vol I.* (1984). Prediction of the diffusion coefficient was done using the Einstein relation which relates the diffusion coefficient to the mean squared displacement of the molecules such that it is equal to the terminal slope of the mean squared displacement curve divided by 6.[2]

The Table 2 gives a comparison of the computed values and their error related to the experimental values (shown in parentheses). For comparison values predicted using a similar simulation setup for the non-polarizable TBP model are also shown. For both polarizable models, the predicted density is within ~2% of the experimental value. The density value for the non-polarizable model is somewhat higher than the one given in the FY09 report—a much longer time average (1ns) is reported here and thus the current value is more representative. The larger discrepancy for the dipole moment predicted by the polarizable model may be due to the

[2] Note, however, that only a single time reference is used rather than an average over many reference times. Thus, the values presented here are preliminary in nature.

larger partial charges on the non-polarizable model (which were taken from Baaden et al 2001[3]) than those used for the polarizable cases. The dielectric constant is poorly predicted by the fixed-charge model as expected, but the first polarizable model is equally poor. The differences in results from the two polarizable models highlight the sensitivity of the model to the assigned charges and polarizabilities. The second version of the model does an excellent job of matching the parameters explored here and provides by far the best estimates for the dipole moment and dielectric constant.

Table 2. Comparison of predicted TBP density and diffusion constant. The colors give an indication of the relative accuracy with green being less than ~5%, yellow ~10%, orange ~50% and red greater than 50% error.

Model	Density, mol/L	%Error (3.652)	Diff. Const.[2], 10^6 cm^2/s	%Error (2.29)	Dipole Moment, D	%Error (3.1)	Dielectric Const	%Error (8.09)
Non-polariz.	3.814 ± 0.020	4.43%	2.05 ± 0.03	-10.5%	4.82 ± 1.23	55.5%	11.75	45.2%
Polariz. V1.1	3.709 ± 0.023	1.56%	3.34 ± 0.03	45.8%	2.39 ± 0.38	-22.9%	3.25	-59.8%
Polariz. V1.2	3.731 ± 0.078	2.16%	2.25 ± 0.01	-1.75%	3.14 ± 0.51	1.29%	8.54	5.6%

[3] Baaden et al. *J. Phys. Chem. B,* **105**:11131 (2001).

Continuum-scale Simulations, Part 1: Advanced CFD Using FELBM

Introduction

Beginning in FY09, collaboration was initiated with Dr. Taehun Lee of the Mechanical Engineering Department of City College of New York on development of an advanced CFD method for application to solvent extraction relevant, multiphase systems. As described in last year's report this method couples an unstructured finite element solution method with the lattice Boltzmann method (FELBM) for solution of the discrete Boltzmann equation on an unstructured mesh.[4] While the method reduces to the Navier-Stokes equations for a slightly compressible limit, it has a significant advantage over traditional CFD methods in that it requires only nearest neighbor information through the collision and streaming step during solution of the particle velocity distributions and it also does not require a global pressure solve of the Poisson equation which is quite costly in traditional CFD. The FELBM method has also been combined with a free energy-based, diffuse interface multiphase method developed by Dr. Lee to enable the free-surface simulations considered here. Simulations were done using the parallel FELBM code provided by Dr. Lee, who also kindly helped make modifications to the code as necessary to improve solution stability—particularly, through implementation of an improved method for velocity boundary condition treatment for the multiphase case. At this time, solution is restricted to relatively low Reynolds number though thorough testing of an already implemented Smagorinsky-type sub-grid scale model for Large Eddy Simulation may broaden the allowable range of Re in the near future.

Geometry and Conditions

The parameters for the simulations are specified in dimensionless units. The simulated geometry had an inner radius of 1.0 and an outer radius of 1.5 resulting in a radius ratio of 0.667; the height of the domain was 4.0. This configuration was selected as it allows direct comparison with the experimental observations of Watanabe et al 2005.[5] The mesh consisted of 1.2M hexahedral elements with 30 elements in the radial direction and 200 each in the axial and azimuthal directions. The initial height of the stationary liquid surface was 2.5. Simulations were conducted for Reynolds numbers (based on the gap width) of 1250, 1500, and 2000 with corresponding Weber numbers of 347, 500, and 888, respectively. According to the experiments of Watanabe et al., it was anticipated that relatively smooth flow would be seen for the lowest Re and increasing to the highest Re traveling surface waves would become evident. Observation of these waves would provide a check of the validity of the modeling methods. Computations were performed on a SiCortex SC5832 HPC system at Argonne having 5832, low-power processing cores each with a speed of only 633 MHz. The FELBM code was found to perform quite well on this machine and all simulations were done using 960 cores (1250 elements/core). Each was run to a time greater than ~10 rotations of the inner cylinder.

Results

The in-plane velocity vectors for a vertical plane showing the counter-rotating Taylor-Couette vortices for the Re 2000 case after ~11 rotations are shown in Figure 6. Five stable vortices are evident. As expected there is some disturbance of the upper vortex by the motion of the free surface. Surfaces waves propagating outward from the rotor are also evident. These waves appear after the first several rotations, but without extending the simulation it is unclear if they

---

[4] Lee and Lin. *J. Comp. Phys.* **171**:336 (2001).

[5] Watanabe et al. *Journal of Physics: Conference Series*, **14**:9-19 (2005).

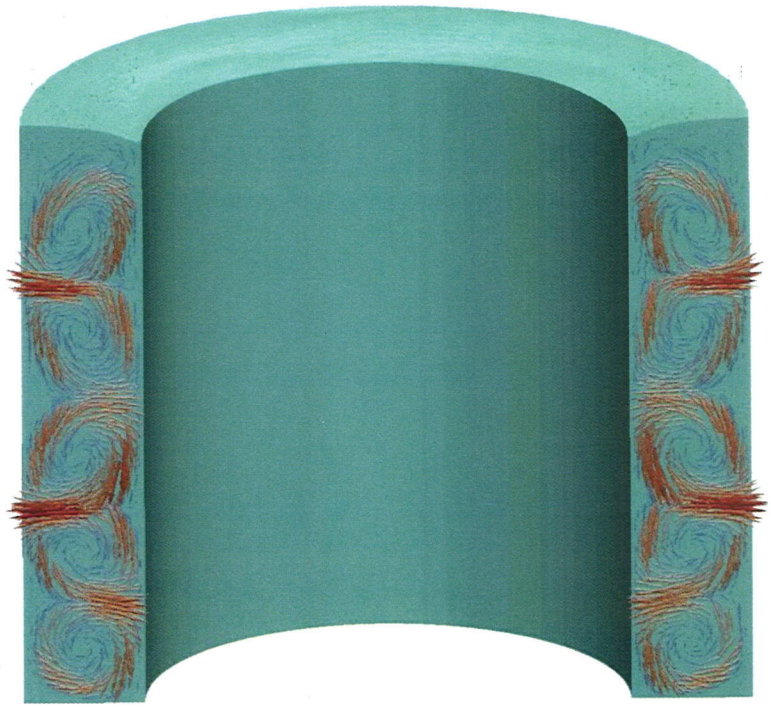

Figure 6. Image showing liquid surface and in-plane velocity vectors on a vertical cross-section for the case at Re = 2000 after a simulation time equivalent ~11revolutions.

will continue to grow; comparison with the experimental observations of Watanabe suggest that they should.

Figure 7 shows an overhead view of the liquid surface for the three different Re after approximately 10 rotations showing a more clear view of the surface waves for each case. In order to highlight these surface undulations, the surface is colored by elevation with red being high and blue low. As was found in the experiments of Watanabe, the flow is quite smooth for the lower Re and surface waves begin to appear for the two higher Re. This good comparison with the experimental observations lends confidence to the general validity of the simulation methodology.

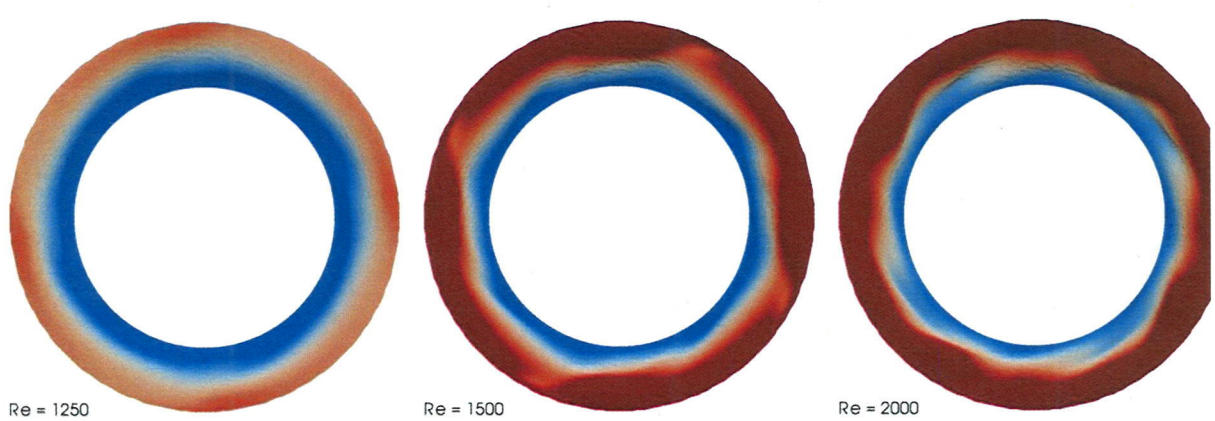

Figure 7. View of liquid surface colored by elevation showing surface waves for the three Re at ~10 revolutions.

Several conclusions can be drawn from our experience to-date with the FELBM code. Firstly, the parallel performance is indeed excellent and the code performs quite well down to ~1000 elements/processor. One current bottleneck for performance is the size of the data files—which are significantly larger than traditional CFD due to the multiple velocity components (19 in this model) which are used—and the corresponding long write times for snapshots. Improvement of the I/O methods in the code is a top priority and several algorithms are being considered. The current 'low' Reynolds number restriction is also prohibitive and additional evaluationg of an LES sub-grid turbulence model is needed. In general, it seems that the area in which such a method can have the largest impact, rather than as a replacement to traditional CFD methods on the equipment-scale, is as a tool for sub-grid model development through highly refined DNS-like multiphase simulations. Such a tool could be used for exploration and development of droplet models including breakup and coalescence which will be needed for the large-scale simulations where droplet level physics cannot be resolved. In this area, it can have a significant advantage over traditional CFD methods as its high computational efficiency allows exploration of greater physical detail.

Continuum-scale Simulations, Part 2: Open-Source CFD of Contactor Equipment

Introduction

The IPSC development effort under the SafeSeps portion of NEAMS is focused on construction of a combination of simplified models which can be used to predict the dynamic behavior of an entire fuel processing facility. Such high-level models must be informed by detailed experiments and/or simulations in order for them to be physically accurate. One key parameter with wide uncertainty is the extraction efficiency of a given stage in a process. The stage efficiency can vary considerably with process flow conditions having a significant impact on the distribution of critical components in the process. Currently, without costly testing at specific process conditions only conservative estimates can made based on historical experience. Thus accurate, predictive knowledge of this parameter through simulation is of real importance to the success of the IPSC effort in regards to process performance and product monitoring. Prediction of stage efficiency requires accurate evaluation of the liquid-liquid interfacial area and mass transfer kinetics for process components under any conditions—both quite challenging—though advanced simulation techniques are available which can provide a basis for the necessary developments. Beyond this, such tools can broaden our understanding of the flow behavior in solvent extraction devices and enable optimization of design and operation of these critical pieces of process equipment. The current focus of this effort is on the annular centrifugal contactor as this device has a number of vital advantages over other process equipment that make it the prime process component for advanced fuel recycling technologies.

Some results from FY10 efforts at simulation of three-phase, liquid-liquid-air simulations in the centrifugal contactor are given here. Simulations were performed using solvers developed with the open-source CFD package OpenFOAM using the Volume of Fluid (VOF) interface capturing method along with Large Eddy Simulation (LES) for turbulence.

Three-phase, Water/Oil/Air Mixing Zone Simulations

The volume of fluid methodology has been successfully used previously for two-phase water/air simulations of the centrifugal contactor and was also directly applied here to the three-phase water/oil/air case. The purpose here was not to achieve a fully predictive simulation for liquid–liquid mixing and interfacial area; rather, the goal was to demonstrate the limits of such methodology for just those targets. It is reasonably well established through both experiment and reliable theory that the droplet size for a typical organic/aqueous system in a centrifugal contactor under typical conditions is in the vicinity of 25 microns with individual droplets as small as just a few microns. The mesh spacing used for this simulation, while ~2X finer than any used previously, still only achieves a minimum spacing of 0.25 mm meaning that it will not be possible to resolve droplets any smaller than those on the order of 1 mm. Even so, the simulations are insightful for exploring general aspects of the bulk flow and also can demonstrate the need for developing advanced multiphase models to achieve the aims of this effort.

Snapshots of the phase volume fractions as seen from the side and for a cross-section are shown in Figure 8. While some small, under-resolved droplets with a characteristic size on the order of the grid spacing are indeed observed, in general the two phases remain in larger globules and rivulets and a 'uniform' dispersion is not observed. It can be seen from Figure 8(b) that with respect to the air, the two liquid phases act almost as a single 'fluid' as has been pointed out previously from simple 2D axisymmetric simulations. This observation, along with the fact that

one cannot hope to be able to fully resolve all the droplets of a fine liquid-liquid dispersion on a mesh using VOF, leads to the conclusion that advanced multiphase methods which couple VOF for liquid/air interface capturing and allow for Eulerian–Eulerian dispersed phase mixing between the two liquids with statistical treatment of droplets may be a successful route towards simulation of solvent extraction processes in these devices.

Three-phase, Water/Oil/Air Coupled Mixing/Separation Zone Simulations

Previously, simulations of the centrifugal contactor have been done in a segregated manner using separate geometries and simulations for the mixing[6] and separation[7] zones. However, such treatment is not ideal as it necessitates specification of a boundary condition for the rotor inlet surface which serves as the outlet to the mixing zone and the inlet to the separation zone. Specification of this boundary condition, particularly for the pressure on the mixing zone outlet, is somewhat problematic. Thus, a successful effort was made this FY to conduct a coupled zone simulation of the centrifugal contactor using OpenFOAM. The results of three-phase water/oil/air simulations using VOF are briefly described here. As noted in the previous section, it is acknowledged that the VOF method alone cannot provide an accurate prediction of the liquid-liquid interfacial area even with highly resolved meshing. However, these simulations provide useful insight and a basis for needed future developments.

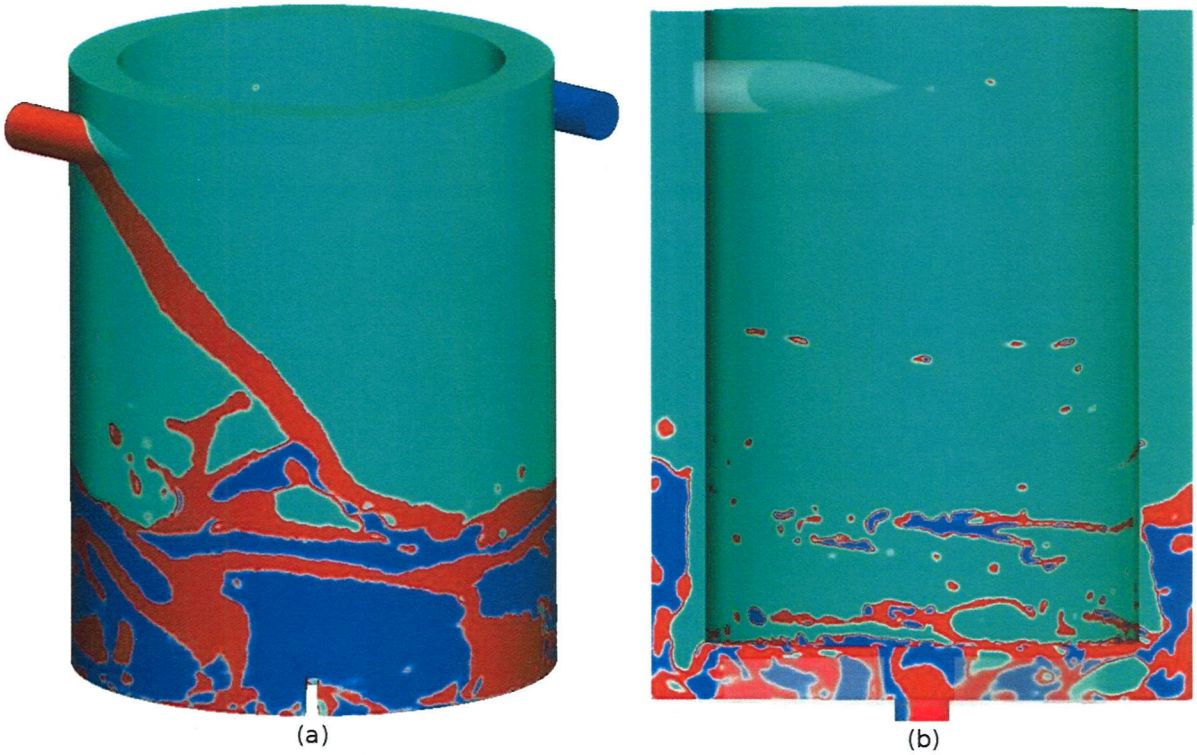

Figure 8. Snapshot of phase distributions for water (blue), oil (red), and air (cyan) for (a) the housing side and (b) a vertical cross-sectional plane and on the rotor. While there appears to be a thin layer of red in regions bordering blue and cyan, this is merely an artifact of the continuous coloring method used for plotting the three phases.

---

[6] Wardle et al. *AICHE J.* **55**:2244-2259 (2009).
[7] Wardle et al. *Sep. Sci. Technol.* **44**:517-542 (2009).

Starting from a volume-equilibrated simulation of the coupled-zone geometry for water and air, the inflow at one of the inlets was replaced with organic at double the rate of the water flow making an organic-to-aqueous flow ratio (O/A) of 2. This was primarily done to decrease the fill time required for the organic phase to reach an equilibrium volume in the device. Figure 9 shows a plot of the per zone phase volumes as a function of time after startup showing the equilibration of the flow volumes. The simulation was run to a relatively long flow time—about 48 hours of real time were required for each second of flow time—and it is seen that volume equilibration of the two phases was achieved after ~10s of flow. It can be seen from the time delay for the oil phase to begin entering the rotor (dashed red line) that the residence time in the mixing zone is ~2-3s.

Snapshots of the phase distributions in the contactor are shown in Figure 10(a) and 10(b). The annular column of the oil phase (red) layered atop the water phase within the rotor can be seen in both views but more clearly on the vertical cross-section in Figure 10(b). Some oil droplets flowing out the light phase exit channels can also be seen in Figure 10(a). Large air pockets in the center of each of the four regions between mixing vanes beneath the rotor are also evident. The total liquid volume in the mixing zone is somewhat less than for the mixing zone only case (compare to Figure 8(b)). This may be somewhat due to the mesh dependency of the VOF methodology, but is certainly also a product of having eliminated the need for explicit specification of the rotor inlet pressure which for the standalone mixing zone case is a key driver for the resulting liquid volume. In this case the volume is allowed to freely respond to the conditions in the device. These simulations were completed near the end of FY10 and further analysis of the results is ongoing.

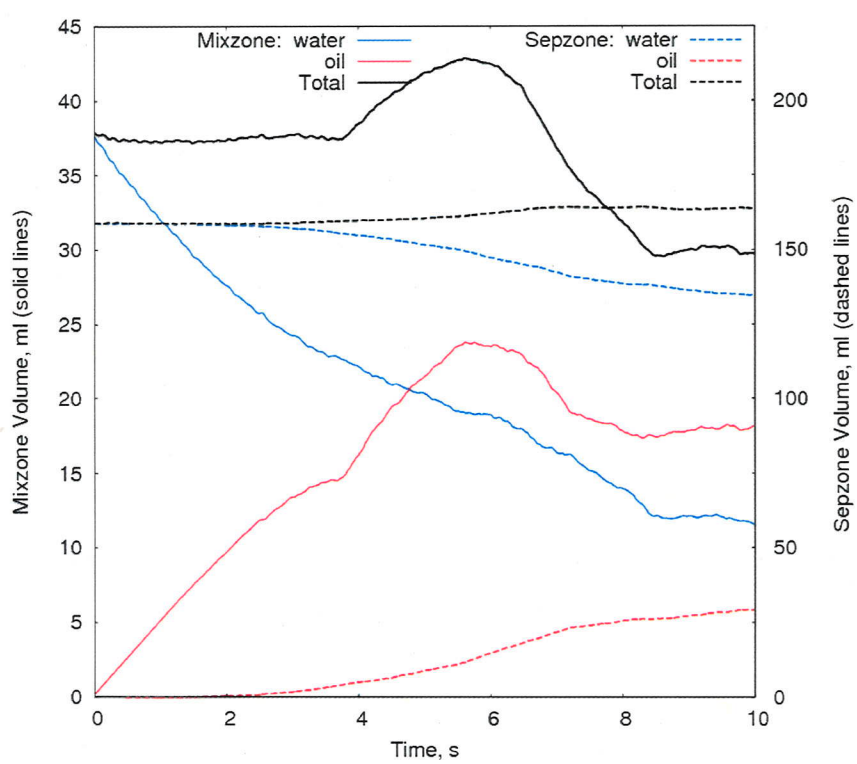

Figure 9. Plot of phase volumes by zone as a function of time after startup (start of inflow of oil phase into previously equilibrated single liquid system).

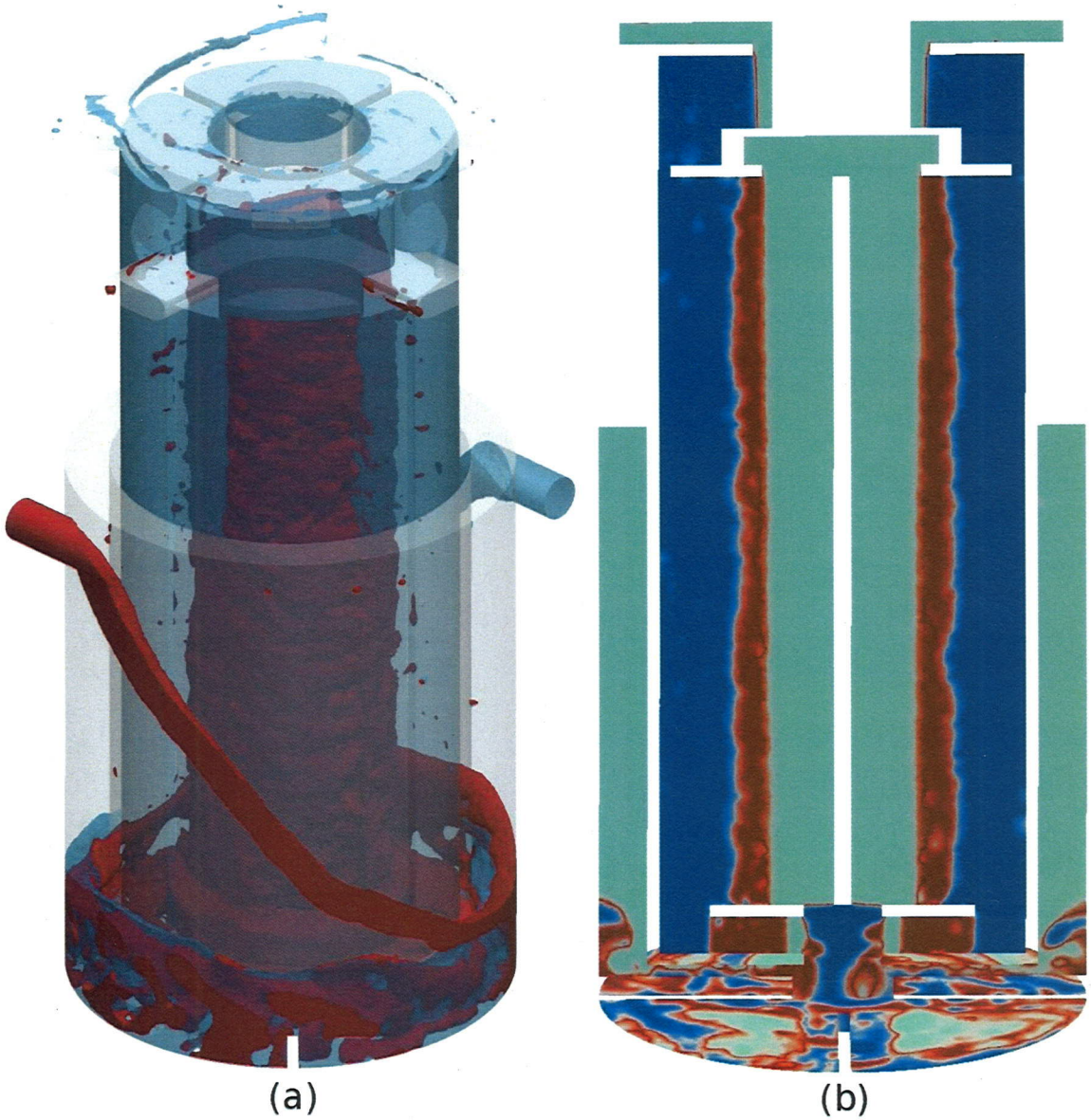

Figure 10. Snapshots of (a) water [blue, transparent] and oil [red] liquid surfaces in the full volume of the coupled-zone contactor model and (b) phase fractions on a vertical cross-sectional plane within the rotor and a horizontal one below the rotor in the mixing zone (air is shown as cyan). As noted in regard to Figure 8, the thin red layer in the upper heavy-phase section of (b) and elsewhere is simply an artifact of the continuous coloring scheme used for the three phases and not an actual layer of oil.

Conclusions

It is clear from these simulations that while the VOF methodology is capable providing a general idea of the flow in both regions of the contactor, the mesh required for full resolution of the inter-phase mixing and resulting small droplets is computationally prohibitive even with massive HPC systems due to the fine meshing and very small time steps that are required. An interpenetrating, statistical multiphase modeling methodology coupled with VOF for the liquid/air interface(s) should be employed to enable prediction of the physical effects of the unresolved droplet scales. Such work will be the main focus of the FY11 efforts in this area.

Chemical Sciences and Engineering Division
Argonne National Laboratory
9700 South Cass Avenue, Bldg. 205
Argonne, IL 60439

www.anl.gov

Argonne National Laboratory is a U.S. Department of Energy
laboratory managed by UChicago Argonne, LLC